PART Ⅱ

PART Ⅱ Result of the First Year's Investigation

Chapter 1 Satellite Image Analysis

1.1 Objective and Area for Satellite Image Analysis

The objective of the satellite image analysis is to regionally interpret geological structure and lithology of the Project Area in order to provide background information for airphoto interpretation and geological prospecting.

The area for image analysis is bounded by lines connecting the four corner points, of which coordination is indicated in Table 4, and occupies an area of approximately 550 km^2. Its location is illustrated in Figure 5.

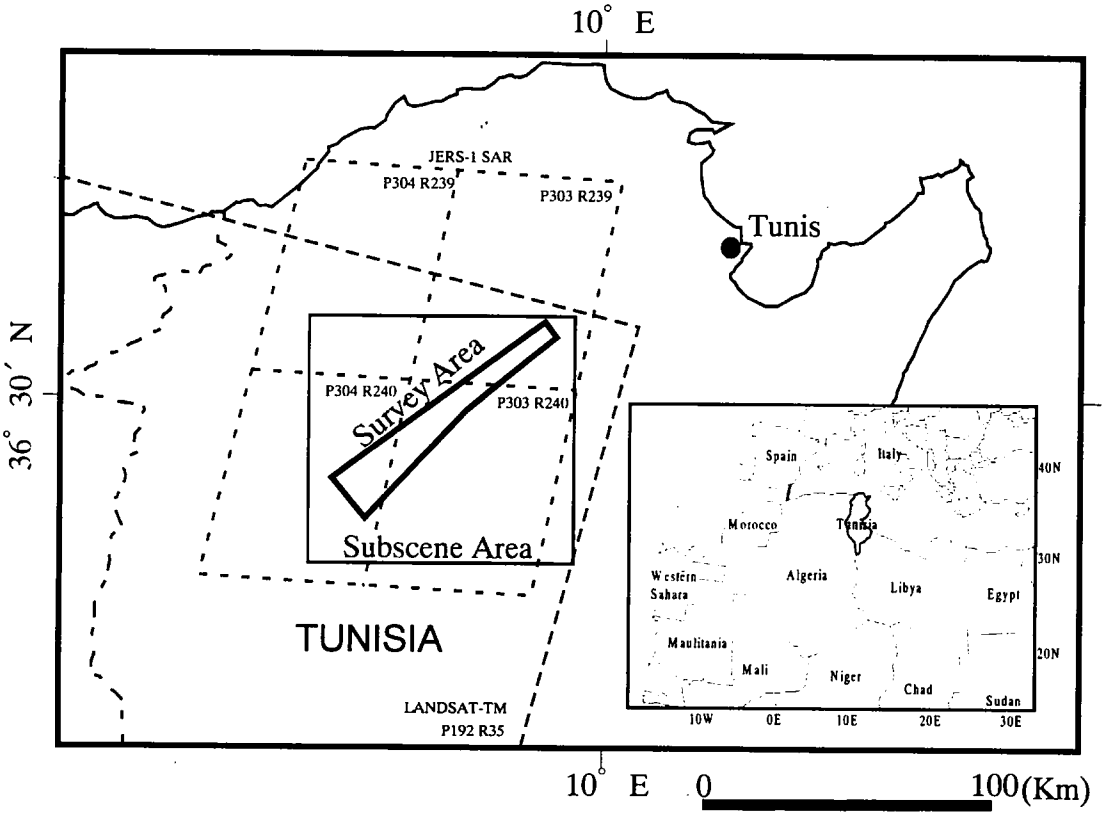

Figure 5 Satellite image location map

Table 4 Area of Satellite Image Analysis

Corner Point	Longitude	Latitude
Northwest	9° 40' 10.3" E	36° 39' 05.0" N
Northeast	9° 43' 02.6" E	36° 36' 13.9" N
Southwest	9° 03' 10.4" E	36° 39' 03.4" N
Southeast	9° 10' 24.6" E	36° 39' 44.6" N

In the data processing of image analysis, emphasis is placed on effective identification of lineaments and differentiation of lithology so that the result of the analysis enables the airphoto interpretation to adequately identify geological features related to mineralization of interest. Methodology for the data processing will be explained later in this chapter.

1.2 Landsat-TM Image Analysis

1.2.1 Principles of Rock and Mineral Discrimination

Most minerals constituting rocks and ore deposits display their diagnostic features of spectra in visible infrared (VIR), shortwave infrared (SWIR) and thermal infrared (TIR) regions in the electromagnetic spectrum range, when they encounter incident energy of sunlight. It is, therefore, theoretically possible to discriminate minerals and rocks by observing characteristic spectra produced by interaction between electromagnetic energy of sunlight and matter such as minerals and rocks. Such diagnostic spectra are generated by effects of electronic transitions in ultraviolet and visible infrared regions, of vibrational molecular transitions in shortwave and thermal infrared regions, and of rotational molecular transitions in far infrared and microwave regions.

Transition metals, such as Fe, Mn, Cu, Ni, Cr and so forth, reflect spectra caused by transitions of electron energy levels when they interact with incident radiation of VIR region. Diagnostic absorption spectra of trivalent iron are observed at wavelengths of 0.35, 0.45, 0.55-0.65 and 0.75-0.95 μm, and those of divalent iron, at wavelengths of 1.0-1.1 and 1.8-2.0 μm.

In SWIR region (1.2-3.0 μm), as above mentioned, mechanism of spectrum generation is attributed to molecular energy level transition by stretching vibration. Minerals display their absorption spectra at different wavelengths depending mainly on their chemical constituents, specifically, such groups as Al-OH, CO_3, Mg-OH, Fe-OH and so forth. Diagnostic absorption spectra are identified at wavelengths of 2.16-2.24 μ

m for minerals containing Al-OH, of 2.3-2.39 μm for those containing CO_3, of 2.3-2.39 μm for those containing Mg-OH, and of 2.24-2.27 μm for those containing Fe-OH. Typical minerals, which indicate diagnostic absorption spectra in SWIR region, are presented in Table 5 for the wavelength ranges of their diagnostic absorption spectra together with chemical constituents responsible for the absorption spectra.

Table 5 Typical Minerals indicating Absorption Spectra in SWIR Region

Constituent Responsible for Absorption Spectrum	Wavelength Range of Absorption Spectrum	Typical Mineral and Mineral Group
Al-OH	2.16-2.24 μm	Kaolinite, Pyrophyllite, Montmorillonite, Alunite, Muscovite/Sericite, Gibbsite
Mg-OH	2.3-2.39 μm	Serpentinite, Talc, Biotite, Chlorite, Hornblende
Fe-OH	2.24-2.27 μm	Jarosite
CO_3	2.3-2.39 μm	Carbonates
H_2O	2.0-2.5 μm	Gypsum, Zeolite

In TIR region (7.0-15.0 μm), thermal emission from the earth's surface is the main source of electromagnetic energy for spectrum generation rather than incident radiation of sunlight. Spectra are generated by molecular energy level transition due to deformation vibration. Major rock forming minerals, such as quartz, feldspars and other silicates, display their diagnostic absorption spectra in this wavelength region. Spectral characteristics of silicates are summarized as follows;

1) Within the wavelength range of 7.0-9.0 μm, the maximum emissivity, 'Christiansen Peak', shifts its position from the shorter wavelength side to the longer wavelength side with decreasing proportion of SiO_2 in rocks. In other words, basic rocks exhibit the Peak at longer wavelengths than acidic rocks.
2) Within the wavelength range of 8.5-12.0 μm, the minimum emissivity shifts its position from longer wavelength side to shorter wavelength side with increasing degrees of SiO_4 condensation. In other words, tectosilicates among other silicate groups exhibit their minimum emissivity at the lowest wavelength, while nesosilicates with the least degree of SiO_4 condensation, at the highest wavelength.
3) Within the wavelength range of 12.0-15.0 μm, absorption spectrum is observed only for tectosilicates but not for any other silicate groups.

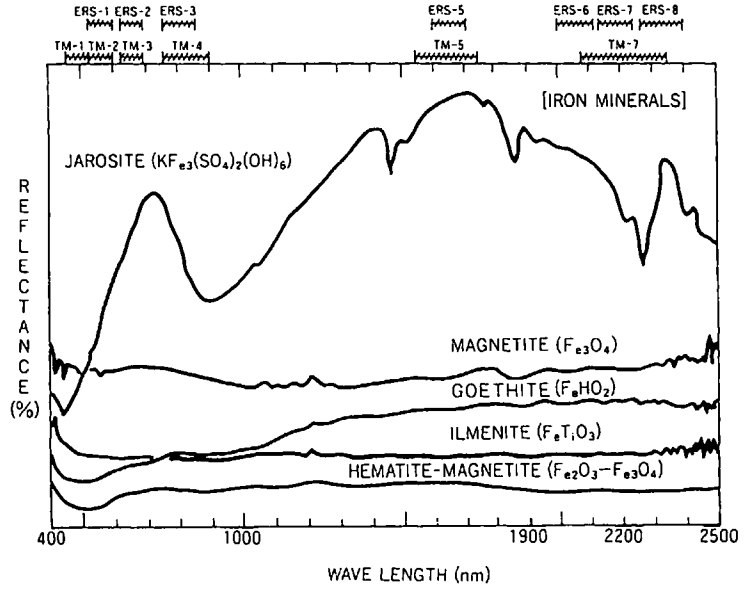

Iron oxides

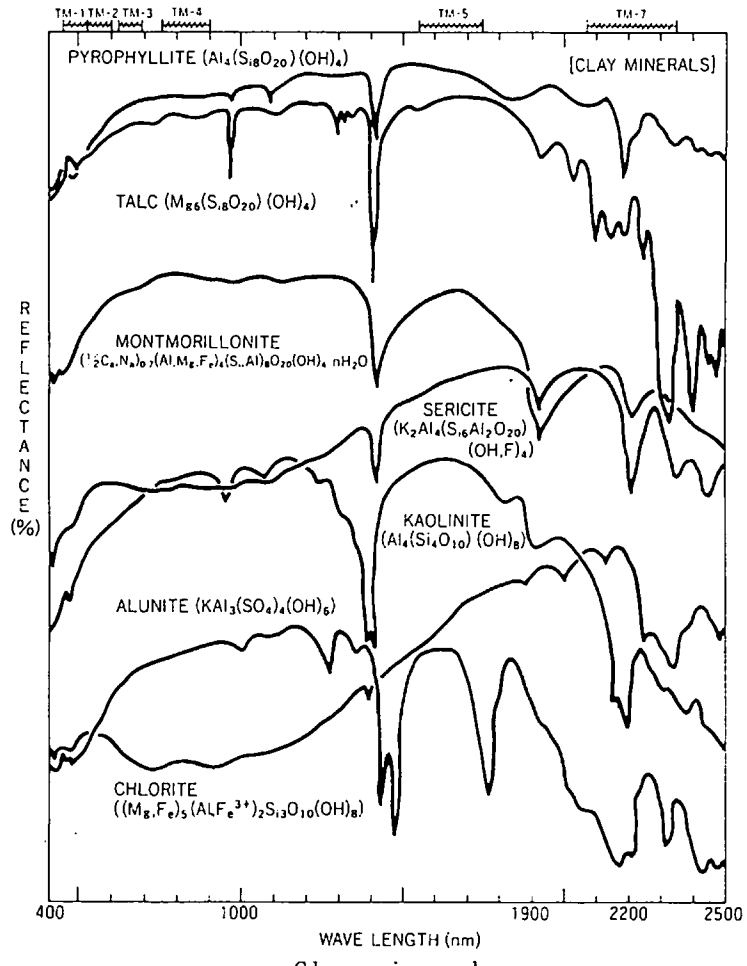

Clay minerals

Figure 6 Spectral patterns of iron oxide and clay minerals

Although the theoretical background for rock and mineral discrimination is explained as above, the data set of Landsat-TM is limited in its capability for application to rock and mineral discrimination mainly due to insufficient spectral resolution of bands. For example, the band 7 of SWIR region, with its spectral resolution of 0.27 μm or 270 nm, is incapable of differentiating clay minerals but collectively detects them as 'total clay'.

1.2.2 Data and Image Processing

(1) Data

Specifications of Landsat-TM data, which are used for the image analysis, are presented in Table 6. The data have been acquired in a month of the dry season (September), when vegetation activity is minimal in a year. Landsat-TM observation parameters are presented in Table 7.

Table 6 Landsat-TM Data Specifications

Sensor	Path	Raw	Date of Data- Acquisition
Landsat-TM	192	35	Sep. 13, 1987

Table 7 Landsat-TM Observation Parameters

Band	Wavelength Range (μm)	Spatial Resolution (m)	Swath (km)
1	0.45-0.52	30	185
2	0.52-0.60	30	185
3	0.63-0.69	30	185
4	0.76-0.90	30	185
5	1.55-1.75	30	185
6	10.40-12.50	120	185
7	2.08-2.35	30	185

The Landsat-TM data comprises multi-spectral images of 4 bands in visible infrared region (bands 1 through 4), 2 bands in short wave infrared region (bands 5 and 7) and 1 band in thermal infrared region (band 6).

Since trivalent iron displays its absorption spectra in VIR region as

aforementioned, the bands 1 through 4 are effective to detect iron oxides such as hematite, jarosite, goethite and limonite. In particular, reflectance of these minerals is invariably low in the band 1 wavelength range of 0.45-0.52 μ m in comparison with that of other minerals. The band 7 with the wavelength range of 2.08-2.35 is effective to detect clay minerals and carbonates inclusively, though differentiation of these minerals is conditional.

(2) Image Processing

Map projection parameters, which are used for georectifying Landsat-TM data sets, are presented in Table 8.

A sub-scene comprising 2,685 pixels x 2,628 lines, which includes the area for image analysis, is framed out of a full scene of Landsat-TM image after the full scene data sets are georectified. The sub-scene data sets are used for generating various false color and principal-component images.

Table 8 Map Projection Parameters

Coordination System	UTM
UTM Zone	32
Center Longitude of Zone 32	9.00000° E
Projection	Transverse Mercator
Earth Model	WGS84
Sub-scene Coordination (UTM)	
Upper Left	500,000.000E, 4,057,938.798N
Lower Right	575,277.425E, 3,984,270.969N

1.2.3 False Color Image

(1) RGB = 3.2.1 (Figure 7)

This image is produced by assigning three primary additive colors, red, green and blue to Bands 1, 2 and 3 respectively. This band combination is recommended by RESTEC (Remote Sensing Technology Center) for a true color image which presents colors of objects close to those sensed by human eyes. The image of the Project Area expresses vegetated lands in black or dark brown, bare grounds in white, light green or light brown, and cultivated lands in brown, light brown or light gray. Although topographic features and geological structures can be recognized on this image, lithological differentiation is very difficult.

Figure 7 False color composite image of Landsat-TM image (RGB=3・2・1)

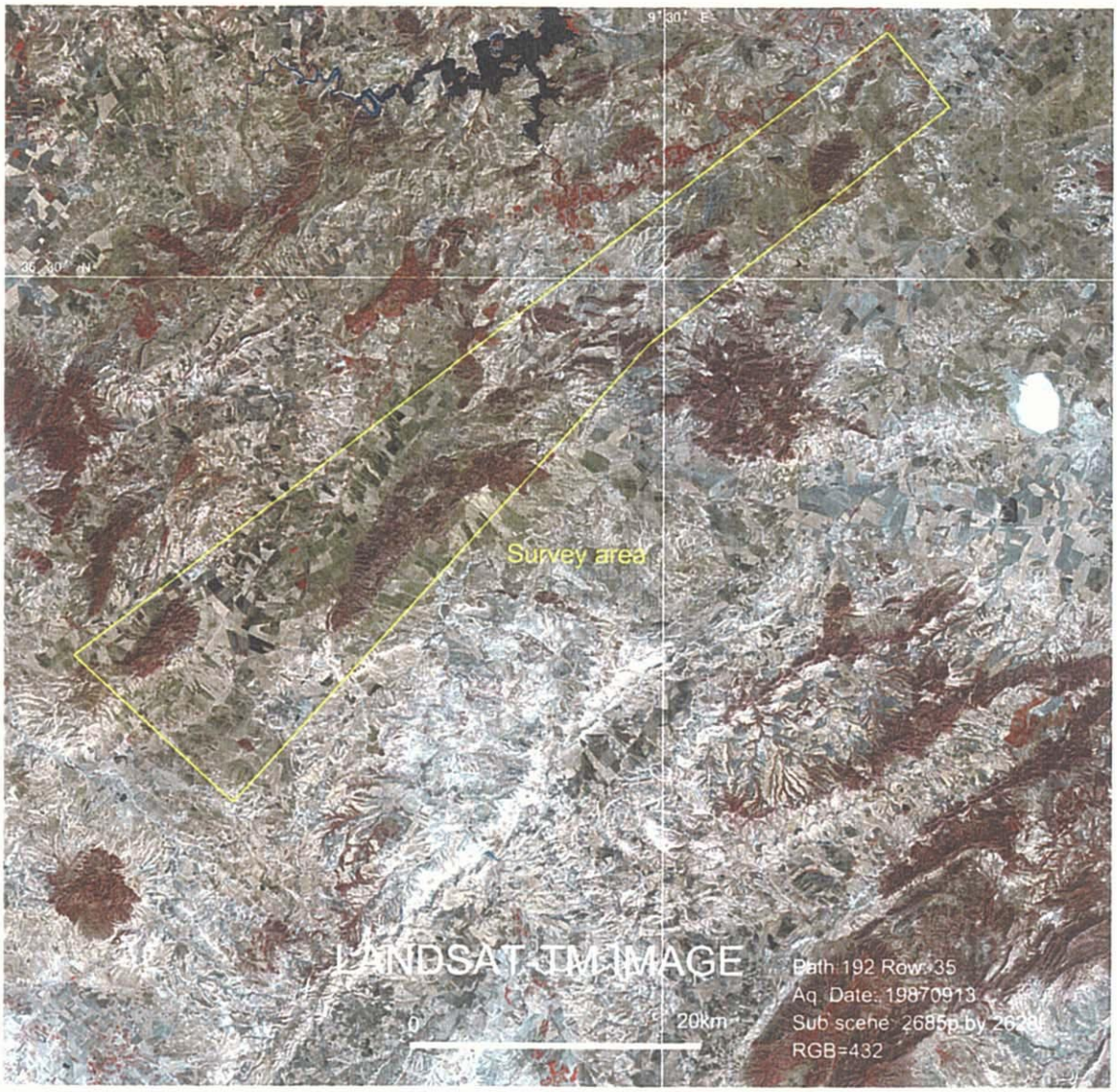

Figure 8 False color composite image of Landsat-TM image (RGB=4·3·2)

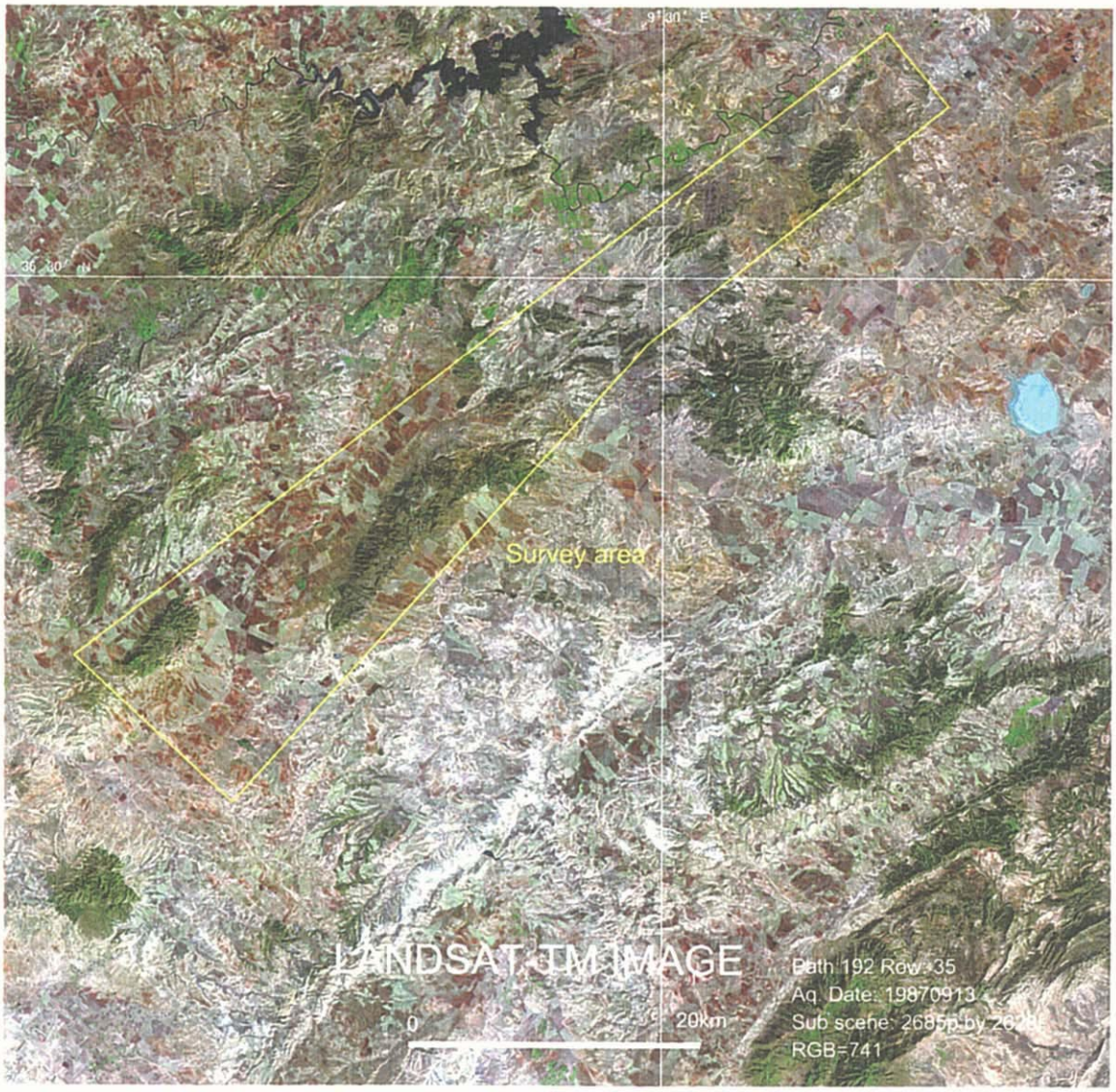

Figure 9 False color composite image of Landsat-TM image (RGB=7·4·1)

(2) RGB = 4.3.2 (Figure 8)

Red, green and blue are respectively assigned to Band 4, 3 and 2 in this false color image. The band combination is one of those for ready-made false color images supplied by RESTEC and is known of its fair expression of topography, vegetation and geographic features. The image of the Project Area shows red to reddish brown color along river and streams, over hills and on residential areas, where vegetation is relatively thick. Lithology is difficult to be differentiated on this image, although it is possible to recognize vegetation, topography and geological structures.

(3) RGB = 7.4.1 (Figure 9)

The combination of Band 7, 4 and 1, to which red, green and blue are respectively assigned, is designated for generating a false color image which makes it possible to distinguish clay alteration zones, carbonate rocks and iron oxide zones. Band 7 will provide spectral features specific for clay minerals and carbonates, while iron oxides can be identified by combination of spectral features in Bands 1 and 4. This image is generated by adding Band 7 (2.08—2.35 μm) of SWIR region to the two bands (Bands 1 and 4) of VNIR region, and presents a variety of color features in comparison with the above two images (Figures 5 and 6) generated by three bands only of VNIR region. For example, hills on the image indicate variable colors, such as green, dark green, purple, yellow, light green, light gray and so forth, which may reflect differences in lithology. Topography, geological structures and land uses can be also recognized on the image.

1.2.4 Principal Component Image

The main purpose of principal-component analysis is to compress a huge volume of complex multi-spectral data into three major groups of correlative data (principal components), in order to express a number of factors by three primary additive colors, namely, red, green and blue (RGB). Data of Bands 1 through 5 and Band 7, excluding those of Band 6, are used for the principal-component analysis. The results are indicated in Table 9 and 10.

Table 9 Eigenvalues and Contributions of Principal Components

Eigenchannel	Eigenvalue	Deviation	Contribution
PC-1	3308.2209	57.5171	90.84 %
PC-2	224.3998	14.98	6.16 %
PC-3	71.4512	8.4529	1.96 %
PC-4	22.8297	4.778	0.63 %
PC-5	12.4711	3.5314	0.34 %

Table 10 Eigenvector Matrix

	Band 1	Band 2	Band 3	Band 4	Band 5	Band 7
PC-1	0.31187	0.23249	0.42717	0.3041	0.65672	0.37633
PC-2	0.49195	0.33167	0.38159	0.29643	-0.51948	-0.38032
PC-3	-0.40257	-0.18396	-0.06769	0.75454	0.20107	-0.43562
PC-4	-0.14969	-0.00997	0.46023	-0.49694	0.36215	-0.62256
PC-5	0.60781	-0.03198	-0.61225	-0.04084	0.34804	-0.36318

The 1st order principal component (PC-1) indicates high positive values in eigenvector for all 6 bands and is high in its contribution at 90.84 %. This implies that PC-1 is related to a spectral feature common for all bands regardless of characteristics of observed grounds and can be attributed to reflectance or albedo of observed grounds. Therefore, PC1 is unsuitable for one of the three principal components for the purpose of spectral characterization of grounds.

The 2nd order principal component (PC2) indicates high negative values in eigenvector for Bands 5 and 7 of SWIR region and high positive values for the rest of bands of VNIR region. A number of clay minerals and carbonates have their characteristic absorption spectra in the Band 7 range, while water bodies and moisture contents of vegetation and soils show relatively low reflectance in the Band 5 range. Therefore, negative scores in PC2 may highlight either water bodies, wet lands, evergreens or areas of clay mineral and/or carbonate concentrations.

The 3rd order principal component (PC3) indicates high negative values in eigenvector for Bands 1 and 7, and high positive values for Band 4. As aforementioned (ref. 1-3-1), Mn and Fe, as well as other transition metals, show diagnostic absorption spectra in the Band 1 range. Since the eigenvector of Band 7 is also highly negative, it is expected that negative scores in PC3 may discern areas of concentrations of Fe, Mn, clay minerals and/or carbonates although water bodies or wet lands are also highlighted. The eigenvector of Band 4 is highly positive, which may be attributed to vegetation.

The 4th order principal component (PC4) indicates high negative values in eigenvector for Bands 4 and 7, and high positive values for Band 3 and 5. Negative scores in PC4 may outline either water bodies/wet lands, bare grounds or areas of clay mineral and/or carbonate concentrations.

The 5th order principal component (PC5) indicates high negative values in eigenvector for Bands 3 and 7, and high positive values for Band 1 and 5. Since vegetation displays a absorption spectrum in the Band 3 range, negative scores in PC5

may outlines vegetated areas as well as areas of clay mineral and/or carbonate concentrations.

There are distributed dolomite, gypsum and rock salt of Triassic, and limestone, sandstone and argillite of Cretaceous to Tertiary in the Project Area. Therefore, PC4 that is characterized by the highly negative eigenvector for Band 7 seems to be most effective for lithological discrimination, specifically for differentiating carbonate rocks. PC3 that includes the highly negative eigenvector for Band 1 may be also useful for outlining dolomite, hence diapir, outcrops with extensive development of Mn and Fe oxides due to weathering.

PC2, PC3 and PC4 are selected for principal-component image production in accordance with the assessment as above described and are assigned to red, green and blue respectively. The produced principal-component image is shown in Figure 10. Topographic features are depressed in the image with albedo (PC1) being removed, which enhances lithology and vegetation instead. In the image, reddish or bluish colors tend to indicate clay minerals and/or carbonates, while greenish colors generally coincides with iron oxides and vegetation.

1.2.5 Photogeologic Interpretation of Landsat-TM Image

Photogeologic interpretation is made on the false color image of RGB = Bands 7, 4 and 1 (ref. 1.2.3 (3)) that seems to best express geology, geological structures and lithology of the Project Area.

As the result of interpretation, 10 geologic units are distinguished. The characteristics of each geologic unit are described below.

(1) Unit T

This unit forms dome structures elongating in the NE-SW dierction in the Project Area and can be easily distinguished from other units, being dark green or dark brown in its tone and medium in its texture (Table 11) in the image. Beddings are also observed in part of the unit. The rocks of the unit are correlated to Triassic sediments, carbonate rocks and evapolites (T) in the published geologic map.

(2) Unit C1

This unit, comprising well bedded rocks that are resitant to erosion, varies from dark green, green, light green, dark gray to purple in its tone and is medium in its texture. These rocks are correlated to Cretaceous sediments (marl etc.) and carbonate rocks (aC2, C1) in the geologic map.

(3) Unit C2

This unit, extensively distributing in the southeastern part of the Project Area,

varies from light green, purple, white to reddish brown in its tone and is fine in its texture. The rocks of the unit are moderately bedded and less resistant to erosion than those of Unit C1. They are correlated to Cretaceous sediments (marl etc., C2-E1, C2) in the geologic map.

(4) Unit P

This unit, distributing in the southwestern part, varies from light green, light brown, light yellow, pink to white in its tone and is medium in its texture. The rocks of the unit are unresistant erosion. Beddings are rarely observed in association with these rocks. They are correlated ot Palaeocene sediments (Cm2-P) in the geologic map.

(5) Unit E

This unit varies from brown, reddish brown, green to dark brown in its tone and is fine in its texture. The rocks of the unit are unresistant to erosion, with poor development of beddings. They are correlated to Eocene sediments (E2-3, aE2-3, E1, aE-1) in the geologic map.

(6) Unit O

This unit is dark green, light brown or purple in its tone and medium in its texture. The rocks of the unit are moderately resistant to erosion, with poor development of beddings. They are correlated to Oligocene sediments (M1, O-M1, O, O1) in the geologic map.

(7) Unit M

This unit varies from light green, light brown, light yellow, pink to light gray in its tone and is medium in its texture. The rocks of the unit are moderately resistant to erosion, with moderate development of beddings. They are correlated to Miocene sediments (M3) in the geologic map.

(8) Unit Pl

This unit is light green, yellow or light yellow in its tone and medium in its texture. The rocks of the unit are moderately resistant to erosion, with poor development of beddings. They are correlated to Pliocene sediments (Pl, M-Pl) in the geologic map.

(9) Unit Qd

This unit, distributing along hill-slopes, is brown or light green in its tone and very fine in its texture. It comprises Quaternary sand dunes (dQ) in the geologic map.

(10) Unit Q

This unit extensively distributes in plains along rivers and water courses and is utilized for crop fields. It varies from brown, pink, green, light green to purple in its tone and comprises Quaternary alluvials (aQ) in the geologic map.

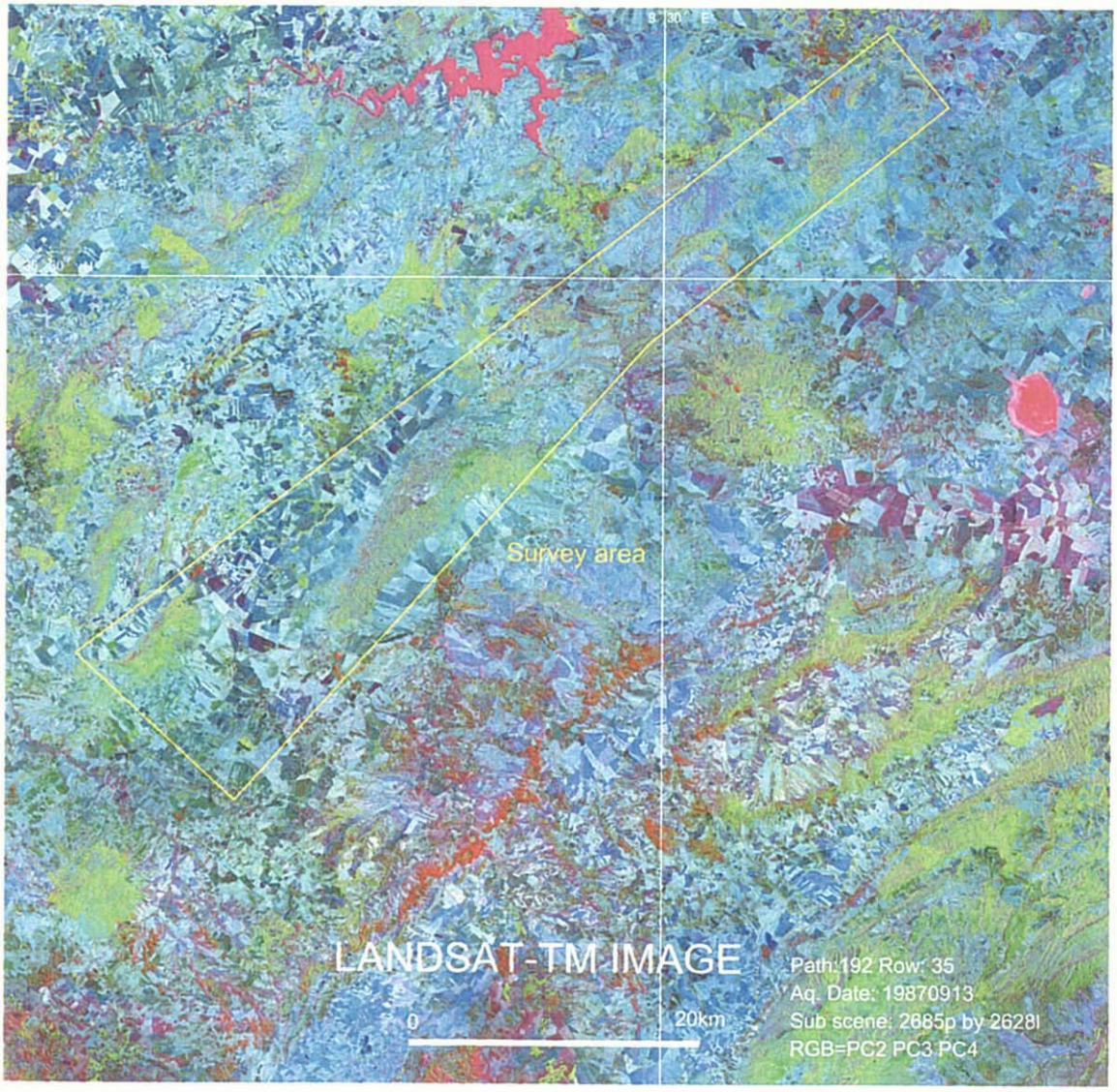

Figure 10 Principal component analysis image of Landsat-TM image (RGB=PC2・PC3・PC4)

Figure 11 Interpretation map for rock phases of Landsat-TM image (RGB=7·4·1)

Figure 12 Interpretation map for geology of Landsat-TM image (RGB=7·4·1)

Table 11 Interpretation chart using Landsat-Tm image (RGB=7,4,1)

Photogeologic units	Image characteristics		Geomorphological features				Correlation with Geologic map (1/500,000)*
	Tone	Texture	Drainage		Rock resistance	Bedding	
			Pattern	Density			
Q	brown, pink, green, light green, violet	none	---	---	---	none	aQ
Qd	brown, light green	very smooth	parallel	low	very low	none	dQ
Pl	light green, yellow, light yellow	intermediate	pinnate	high	moderate	rare	Pl, M-Pl
M	light green, light brown, light yellow, pink, light grey	intermediate	dendritic	moderate	moderate	modetrate	M3
O	dark green, dark brown, violet	intermediate	dendritic	moderate	moderate	rare	M1, O-M1,O, O1
E	brown, reddish brown, green, dark brown	smooth	dendritic	low	low	rare	E2-3, aE2-3, E1, aE1
P	light green, light brown, light yellow, pink, white	intermediate	dendritic	moderate	low	rare	Cm2-P
C2	light green, violet, white, reddish brown	smooth	dendritic	moderate	low	moderate	C2-E1, C2
C1	dark green, green, light green, dark	intermediate	dendritic	moderate	high	well	aC2, C1
T	dark green, dark brown	intermediate	dendritic	high	high	moderate	T

*: MINISTERE DE L'ECONOMIE NATIONALE OFFICE NATIONAL DES MINES DEPARTEMENT DE GEOLOGIE SERVICE GEOLOGIQUE NATIONAL(1985);
CARTE GEOLOGIQUEDE LA TUNISIE ECHELLE 1:500,000

1.3 JERS-1 SAR Image Analysis

1.3.1 Principal Characteristics of SAR Sensor

The SAR (Synthetic-Aperture Radar) sensor is a side-looking radar system, which is capable of acquiring images from satellites at distances of hundreds of kilometers with good spatial resolution. In principle, radar is an active remote sensing system which transmits electromagnetic energy to the earth's surface and detects reflected energy. Radar systems operate in the microwave region of electromagnetic spectrum, ranging from millimeters to meters in wavelength. They can, therefore, operate independently of lighting conditions and are largely unaffected by weather conditions. Synthetic-Aperture is so designated as to successively synthesize energy pulses returning from targets taking advantage of the Doppler principle, which gives a radar system with the effect of a much longer antenna. That is, a satellite equipped with SAR transmits microwave pulses perpendicularly (in range direction) to targets on the earth's surface with moving along its orbit (azimuth direction) and receives returning pulses with changing frequencies according to the Doppler shift during elapsed time from one target to another (Figure 13). The received pulse data are successively sorted and processed in the radar system in order to achieve fine azimuth resolution.

Since a SAR system scans targets on the earth's surface, not vertically but with a certain angle (Off-Nadir or Depression Angle), a geometric distortion, called 'foreshortening' or 'layover', is produced in range directions of radar images. This distortion results in shortening the length of a fore-slope in the range direction compared to its actual length (foreshortening) or in displacement of the top of a tall vertical feature toward the near range (layover). Foreshortening or layover often makes it difficult to adequately read linear features particularly when the terrain becomes steep beyond a certain limit. However, the distortion can be also utilized for generating a DEM (Digital Elevation Model) which is determined in accordance with the relationship between Off-Nadir angles and elevations.

1.3.2 Data and Image Processing

(1) Data

Specifications of JERS-1 SAR data, which are used for the image analysis, are presented in Table 12.

Table 12 JERS-1 SAR Data Specifications

Sensor	Path	Raw	Date of Data- Acquisition
JERS-1 SAR	303	239	10 Sep. 1996
	303	240	10 Sep. 1996
	304	239	24 Jun 1992
	304	240	24 Jun 1992

The smaller the Off-Nadir angle is, the more foreshortening is intensified. The SAR systems of satellites, which were launched in the past, have Off-Nadir angles ranging from 15 to 60° . Therefore, JERS-1 SAR provides radar images with moderate foreshortening in comparison with those of other SAR systems.

Table 13 Specifications of JERS-1 SAR Sensor

Band	1, L band
Frequency	1275 MHz
Spatial Resolution	18 m
Swath Width	75 km
Off-Nadir Angle	35°
Polarization	HH
Orbit Altitude	568 km

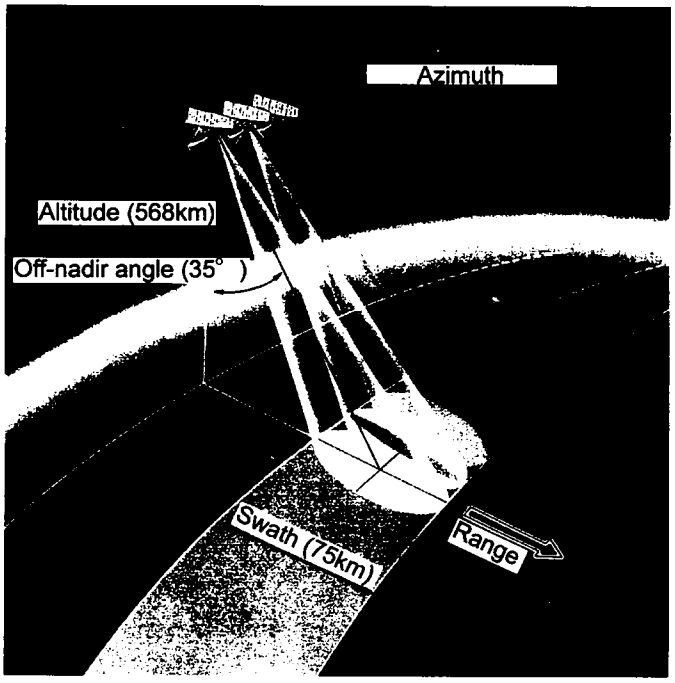

Figure 13 Principal of data acquisition of JERS-1 SAR

(2) Image Processing

Prior to image processing, JERS-1 SAR data are pretreated for edge enhancement using the median filter comprising arrays of three-by-three pixels in order to accentuate linear features in the produced image. The data sets of four JERS-1 SAR scenes, after georectified according to the same map projection parameters as shown in Table 8, are compiled into a single data set for a mosaic by digital mosaicking. A scene comprising

5330 pixels x 5205 lines, which includes the Project Area, is framed out of the mosaic for the photogeologic interpretation.

1.3.3 Photogeologic Interpretation of JERS-1 SAR Image

The JERS-1 SAR Image is shown in Figure 14. In Figure 14, eastern slopes of hills are bright, contrasting with dark opposite slopes, which is resulted from foreshortening of the image with the look direction from the eastern side. Reflection intensity is influenced by backscattering of microwave that depends on roughness of ground surface. Image becomes brighter with increasing roughness. The roughness of the Project Area is dependent mainly on vegetation and lithology. Vegetated hills present bright images, while featureless plains are dark. Vegetation is well developed along water courses, in general, which makes it easier to identify drainage patterns. Water bodies such as lakes and dams are shown in black images due to mirror reflection on their smooth surfaces with nil-backscattering.

The interpreted lineament map is shown in Figure 15. Lineaments are distinct in all the terrain of Triassic, Cretaceous and Tertiary systems. Most predominated are the lineaments in the NE-SW direction, followed by those in the NW-SE and E-W directions in the general area. It is worth to note that the lineaments in the NW-SE direction are dominated in the El Akhouat Adama, Bou Khil, Bazina Kebira and Oued Jebes prospects of the Project Area, where a number of mineral occurrences have been located.

Figure 16 is the composite of the photogeologic interpretation maps using the Landsat-TM and JERS-1 SAR images. The JERS-1 SAR image is unsuitable for discriminating lithology, in comparison with the Landsat-TM image. This is because the Landsat-TM image comprises multi-spectral bands that include various spectral information with respect to lithology. On the other hand, the JERS-1 SAR image provides only information on physiographic features such as surface roughness, drainage patterns and so forth.

The density of lineaments is shown in Figure 17. The density of lineaments tends to be high at the intersections of the lineaments of the NE-SW and NW-SE

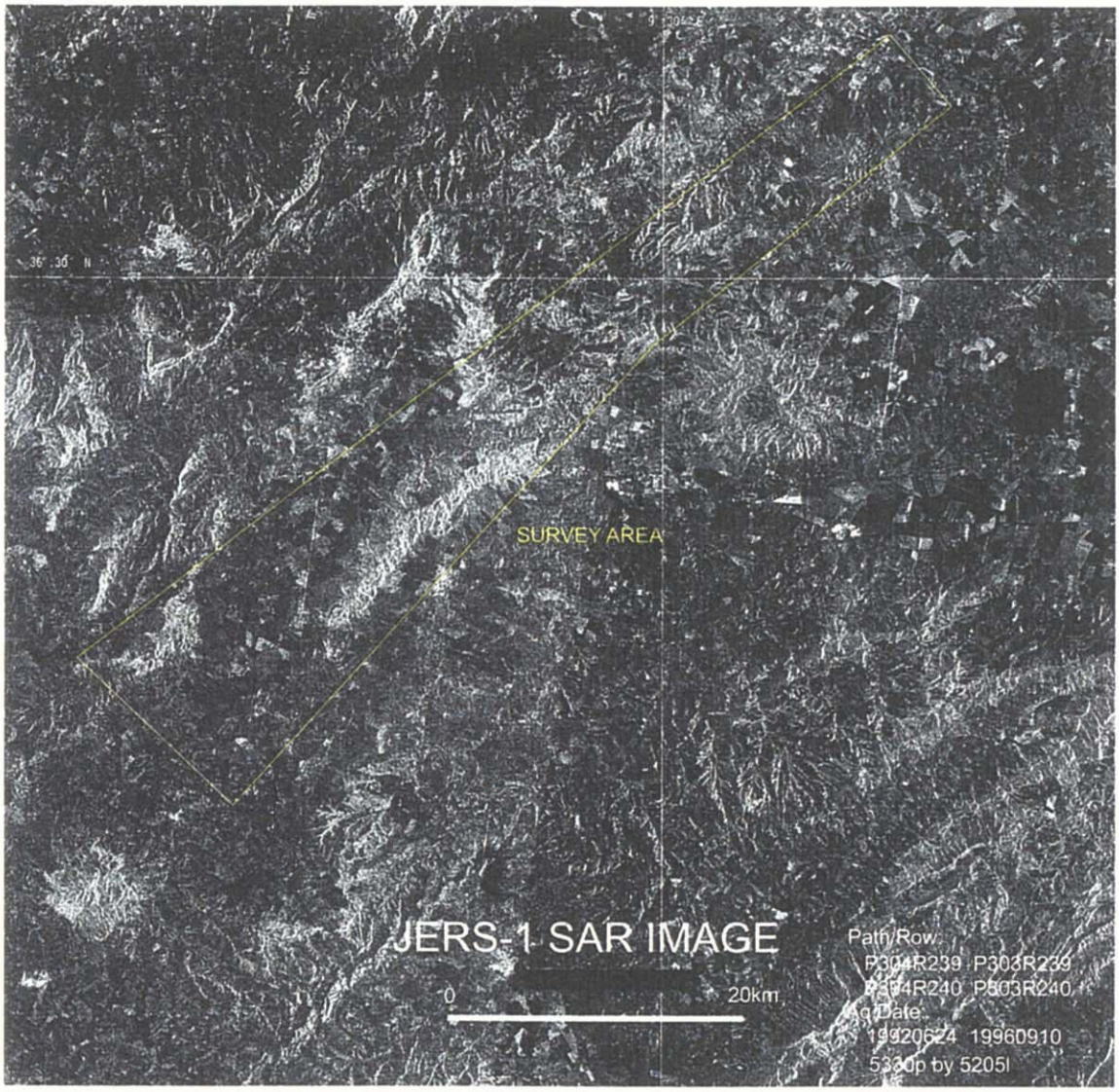

Figure 14 JERS-1 SAR image of the survey area

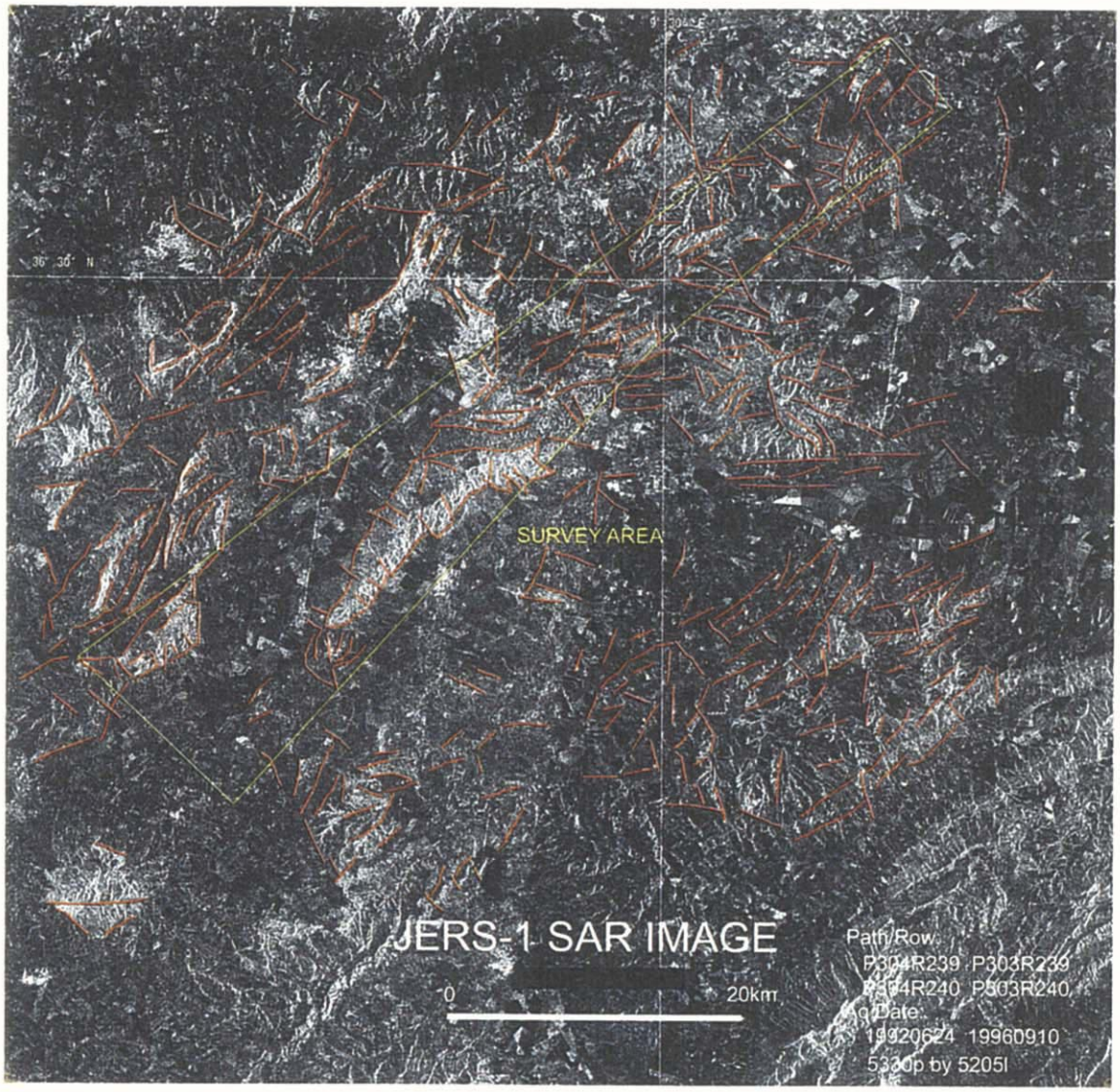

Figure 15 Lineament map of the survey area using JERS-1 SAR image

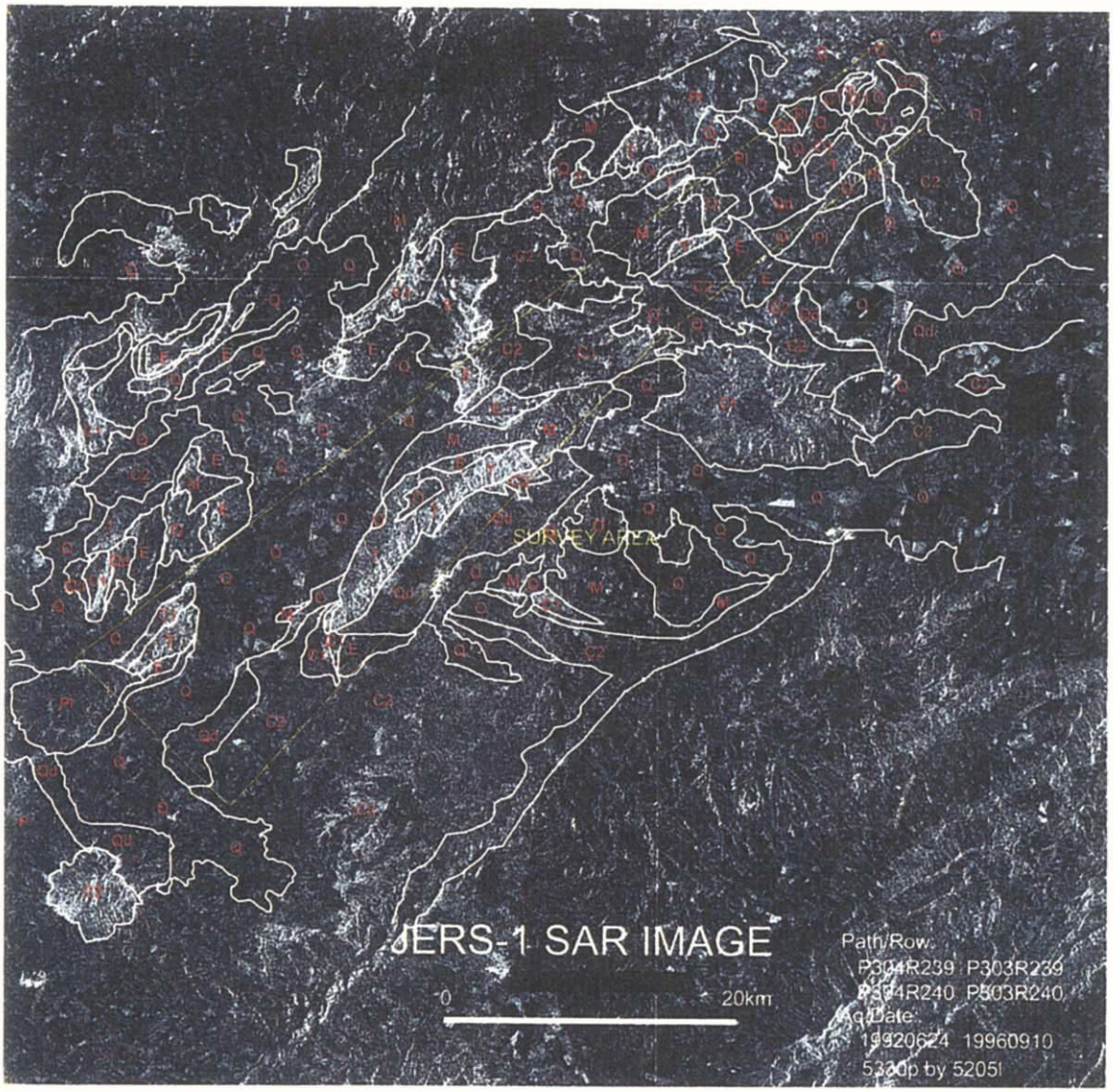

Figure 16 Interpretation map for geological unit

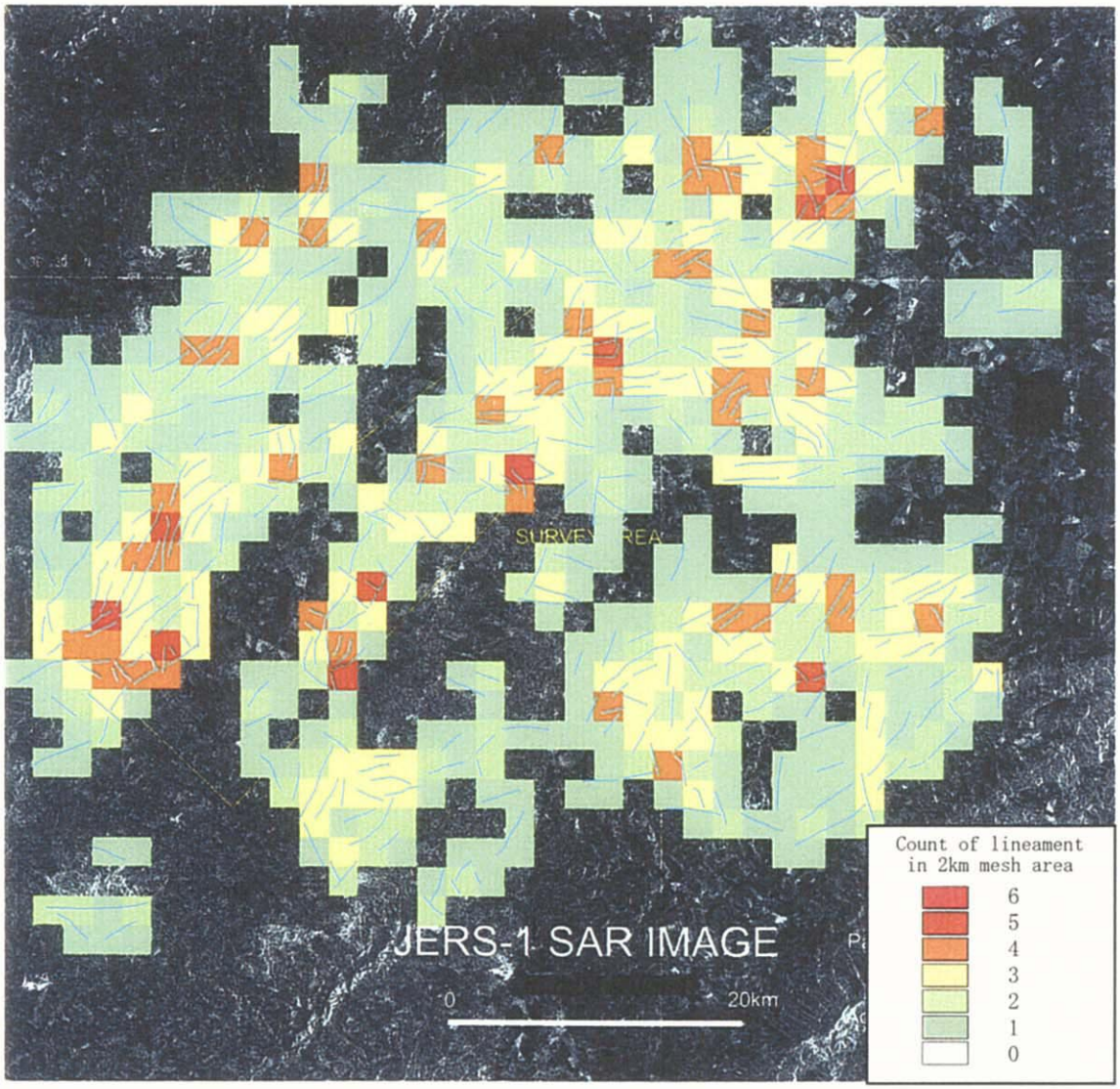

Figure 17 Density map of lineaments

directions crosscutting each other. Areas with high density of lineaments are observed in and around the El Akhouat-Argoub Adama, Bou Khil, Bazina Kebira and Oued Jebes prospects.

The result of photogeologic interpretation of JERS-1 SAR image suggests that potential for Pb-Zn mineralization is high at the intersections between the NE-SW and NW- SE trending lineaments from the locations of known mineral occurrences to the lineaments.